



HAL
open science

A nested circulation model for the North Aegean Sea

V. H. Kourafalou, K. P. Tsiaras

► **To cite this version:**

V. H. Kourafalou, K. P. Tsiaras. A nested circulation model for the North Aegean Sea. *Ocean Science Discussions*, 2006, 3 (3), pp.343-372. hal-00298383

HAL Id: hal-00298383

<https://hal.science/hal-00298383>

Submitted on 18 Jun 2008

HAL is a multi-disciplinary open access archive for the deposit and dissemination of scientific research documents, whether they are published or not. The documents may come from teaching and research institutions in France or abroad, or from public or private research centers.

L'archive ouverte pluridisciplinaire **HAL**, est destinée au dépôt et à la diffusion de documents scientifiques de niveau recherche, publiés ou non, émanant des établissements d'enseignement et de recherche français ou étrangers, des laboratoires publics ou privés.

Papers published in *Ocean Science Discussions* are under open-access review for the journal *Ocean Science*

A nested circulation model for the North Aegean Sea

V. H. Kourafalou and
K. P. Tsiaras

A nested circulation model for the North Aegean Sea

V. H. Kourafalou^{1,2} and K. P. Tsiaras¹

¹Hellenic Center for Marine Research, Anavyssos, Greece

²Rosenstiel School of Marine and Atmospheric Science, Univ. of Miami, Miami, FL, USA

Received: 3 April 2006 – Accepted: 20 April 2006 – Published: 30 May 2006

Correspondence to: V. Kourafalou (vkourafalou@rsmas.miami.edu)

Title Page

Abstract

Introduction

Conclusions

References

Tables

Figures

⏪

⏩

◀

▶

Back

Close

Full Screen / Esc

Printer-friendly Version

Interactive Discussion

Abstract

A multi-nested approach has been employed for numerical simulations in the northern part of the Aegean Sea in the framework of the MFSTEP (Mediterranean Forecast System: Toward Environmental Predictions) project. The high resolution (~ 1.6 km) hydrodynamic model of the North Aegean Sea (NAS) has been nested within a coarser model of the Eastern Mediterranean (resolution ~ 3.6 km) which is also nested within a basin scale model for the Mediterranean Sea (resolution of ~ 7 km). The high resolution of the NAS model allows the representation of topographic details that have never been reproduced in modelling studies of the region. Such details can enhance the simulation of coastal features, but can also influence basin-scale processes, such as the pathways of waters of Black Sea origin inflowing at the Dardanelles Straits and bifurcating through island passages.

We employ comparisons of the North Aegean and Eastern Mediterranean models in terms of computed flow fields and distribution of hydrodynamic properties, to evaluate the nesting procedure, the initialization requirements and the ability of a nested model to perform reliable short term simulations that employ high resolution atmospheric forcing, when initialized from a longer running coarser OGCM.

We show that the topographic details of the high resolution, nested NAS model mostly affect the distribution of the Dardanelles plume, while the imposed high frequency, high resolution atmospheric forcing allows for the formation of an overall energetic flow field after a few days of spin-up period. A longer initialization procedure is suggested for the establishment of stronger currents and better developed buoyant plumes.

1 Introduction

The physical setting of the North Aegean Sea is unique, mainly due to the complex topography of islands, straits, peninsulas and a combination of very shallow and very

OSD

3, 343–372, 2006

A nested circulation model for the North Aegean Sea

V. H. Kourafalou and
K. P. Tsiaras

Title Page

Abstract

Introduction

Conclusions

References

Tables

Figures

⏪

⏩

◀

▶

Back

Close

Full Screen / Esc

Printer-friendly Version

Interactive Discussion

5 deep regions. The North Aegean Trough consists of an extended deep area that forms around three major depressions (maximum depth near 1300 m): the Sporades basin, the Athos basin and the Lemnos basin (Fig. 1). The deep basins separate shelf areas of the Northern Aegean from the generally deeper central basin interior. Examples
10 are the shelf areas to the east and west of the Chalkidiki peninsula, where a number of rivers contribute to the development of coastal currents, which are also triggered by wind forcing. Larger than all the North Aegean rivers combined, is the buoyant inflow of waters of Black Sea origin through the Dardanelles Strait. The development and evolution of the Dardanelles plume is influenced by the presence of neighboring islands and the shallow Lemnos plateau, between the Lemnos and Imroz islands. Other topographic depressions include the Skyros basin and a small area south of the Lesvos island.

15 It is deduced that both the mean flow and the eddy field in the North Aegean Sea will be greatly influenced by the complicated topography, with implications on water mass characteristics and sub-basin exchanges. This is in addition to interactions with the Southern Aegean and with remote and local atmospheric forcing, see Poulos et al. (1997) and Zervakis et al. (2000). Several previous studies have focused on sub-basin observations, mainly addressing seasonal variability, as Balopoulos et al. (1986), Zervakis and Georgopoulos (2002), Kontoyiannis et al. (2003) and Karageorgis et al. (2003). Time series observations are available in a few points, as part of the operational POSEIDON buoy system (Nittis et al., 2002). Studies focusing on North Aegean processes associated with the inflow of buoyant waters of Black Sea origin through the Dardanelles Strait include Zodiatis and Balopoulos (1993), Zodiatis (1994), Zodiatis et al. (1996) and Kourafalou and Barbopoulos (2003).

25 This study is an extension of the model development and numerical simulations of the North Aegean circulation that took place during the Mediterranean Forecast System Pilot Project (MFSP; Pinardi et al., 2003). The North Aegean model that was developed in the framework of MFSP (Kourafalou and Barbopoulos, 2003) had a horizontal resolution of ~ 3 km and was nested within the Aegean and Levantine Eddy Resolving

A nested circulation model for the North Aegean Sea

V. H. Kourafalou and
K. P. Tsiaras

[Title Page](#)[Abstract](#)[Introduction](#)[Conclusions](#)[References](#)[Tables](#)[Figures](#)[⏪](#)[⏩](#)[◀](#)[▶](#)[Back](#)[Close](#)[Full Screen / Esc](#)[Printer-friendly Version](#)[Interactive Discussion](#)

Model (ALERMO) of a resolution of ~ 5.5 km (Korres and Lascaratos, 2003) that was also nested in a basin-wide Mediterranean OGCM of ~ 10 km resolution (Demirov and Pinardi, 2002). In MFSTEP, the same downscaling approach was employed in several areas of the Mediterranean Sea, including the Northern Aegean. The new North Aegean model domain remained the same (north of $\sim 38.5^\circ$ N, see Fig. 1), but horizontal resolution was doubled (~ 1.6 km), following grid spacing decreases in ALERMO (~ 3.6 km) and the Mediterranean OGCM (~ 7 km). The scope of the North Aegean model simulations during MFSP was the study of the seasonal variability; consequently, climatological atmospheric forcing was employed. Here we present the new North Aegean Sea (NAS) model set-up, evaluate the nesting procedure and the ability of a nested model to perform short term simulations under high frequency, high resolution atmospheric forcing, when initialized from a larger scale OGCM. We do not attempt a model validation by comparison to observations (which were not available for the simulation period), but we use the fields of the outer model (ALERMO) as the “truth” and examine if the nested model can reproduce similar circulation features (plus finer details), by relying on the initial and boundary conditions and the detailed atmospheric forcing. This modeling experiment is intended to help develop a suitable strategy for a future operational model of the Northern Aegean Sea.

2 Model description

2.1 Model set-up

The hydrodynamic model implemented in the Northern Aegean is based on the Princeton Ocean Model (POM, Blumberg and Mellor, 1983) which is a three-dimensional, sigma-coordinate, free surface and primitive equation model. POM is a widely spread community model that has been used in numerous applications (details at <http://www.aos.princeton.edu/WWWPUBLIC/htdocs.pom/>). The vertical eddy viscosity / diffusivity coefficients are evaluated according to the Mellor-Yamada 2.5 turbulence

A nested circulation model for the North Aegean Sea

V. H. Kourafalou and
K. P. Tsiaras

Title Page

Abstract

Introduction

Conclusions

References

Tables

Figures

⏪

⏩

◀

▶

Back

Close

Full Screen / Esc

Printer-friendly Version

Interactive Discussion

closure scheme (Mellor and Yamada, 1982) while the calculation of horizontal diffusion is based on Smagorinsky (1963). The model domain (Fig. 1) lies between 22.53° E and 27° E and between 38.63° and 41.03° N. Horizontal resolution is approximately 1/60° (DX~1.4 km, DY=~1.8 km) while 16 (or 25) sigma-levels are resolved in the vertical, with logarithmic distribution approaching the surface. The U.S. Navy Digital Bathymetric Data Base (DBDB1, 1/60° × 1/60°) is used to build the model bathymetry with bilinear interpolation into the model grid; the minimum coastal depth is set at 10 m.

Particular care has been given to the parameterization of riverine and Black Sea inputs. River inflows are modelled as source terms in the continuity equation, based on the plume dynamics study of Kourafalou et al. (1996). This parameterization allows for the development of buoyancy driven circulation that is mainly controlled by the amount of discharge and the interaction with wind stress and topography. All major North Aegean rivers (Evros, Axios, Aliakmonas, Pinios, Strimonas and Nestos) are represented (as 2–6 point sources) in the model. River runoff is set to constant values (same as in Kourafalou and Barbopoulos, 2003), based on climatological annual means (Therianos, 1974). The Thermaikos Bay (Fig. 1) river discharges have been modified according to measurements obtained during the METRO-MED project (Kourafalou et al., 2004). The fresh water is assumed of having zero salinity and seasonally varying temperature. A parameterization different than the imposed net inflow in Kourafalou and Barbopoulos (2003) was adopted for the Dardanelles water exchange regime. The new scheme employs inflow of Black Sea Water (BSW) and outflow of Aegean water i.e., a two layer (inflow-outflow) open boundary condition with prescribed transport rates and BSW salinity (Nittis et al., 2006). In the present study the inflow and outflow transport rates follow a seasonal cycle with maximum values during July (Fig. 2) while BSW salinity is assumed constant (28.3). The depth of the upper layer is assumed to be half of the total water column depth (~25 m). A uniform velocity is calculated for the two layers according to the prescribed inflow/outflow transports. The same scheme was adopted by the ALERMO model.

A nested circulation model for the North Aegean Sea

V. H. Kourafalou and
K. P. Tsiaras

[Title Page](#)[Abstract](#)[Introduction](#)[Conclusions](#)[References](#)[Tables](#)[Figures](#)[⏪](#)[⏩](#)[◀](#)[▶](#)[Back](#)[Close](#)[Full Screen / Esc](#)[Printer-friendly Version](#)[Interactive Discussion](#)

2.2 Nesting procedure

The Northern Aegean Sea (NAS) model has an open boundary to the south where it is nested to the coarser ($1/30^\circ$ by $1/30^\circ$) intermediate model (MFSTEP-ALERMO, http://www.oc.phys.uoa.gr/mfstep/ALERMO_MFSTEP_DETAILS.htm). The intermediate model is at its turn nested to the Mediterranean-wide MFSTEP-OGCM ($1/16^\circ$ by $1/16^\circ$; <http://www.bo.ingv.it/mfstep/>) model. The nesting-approach is one-way, that is, each coarse model influences the solution within the immediate finer one, without any feedback.

The coupling procedure between the NAS and ALERMO models takes into account bathymetry fitting along the nesting boundary and employs the specification of flows and water properties. The NAS model grid and bathymetry along the open boundary are fitted to those of ALERMO in order to minimize interpolation errors for the open boundary input variables. The NAS prognostic fields along the open boundary (total velocity U, V ; barotropic velocity U_a, V_a , temperature T , salinity S , and surface elevation ζ) employ daily averaged ALERMO fields, which are bilinearly interpolated into the model grid and linearly interpolated in time providing lateral input of Velocity (total U_c, V_c and barotropic U_{ac}, V_{ac}), Temperature (T_c), Salinity (S_c) and free-surface elevation (ζ_c) along the open boundary at each model time step. The following open boundary conditions are used:

- An upstream advection scheme is used for T, S when the normal velocity V is directed outwards the model domain. When V is directed inwards, T and S are directly prescribed by the ALERMO model.

$$\frac{\partial T, S}{\partial t} + V \frac{\partial T, S}{\partial y} = 0; \quad V < 0 \quad (1)$$

$$(T, S) = (T_c, S_c); \quad V > 0 \quad (2)$$

A nested circulation model for the North Aegean Sea

V. H. Kourafalou and
K. P. Tsiaras

Title Page

Abstract

Introduction

Conclusions

References

Tables

Figures

◀

▶

◀

▶

Back

Close

Full Screen / Esc

Printer-friendly Version

Interactive Discussion

A nested circulation model for the North Aegean Sea

V. H. Kourafalou and
K. P. Tsiaras

Title Page

Abstract

Introduction

Conclusions

References

Tables

Figures

⏪

⏩

◀

▶

Back

Close

Full Screen / Esc

Printer-friendly Version

Interactive Discussion

- The baroclinic velocities are exactly prescribed by Alermo velocities:

$$(U, V) = (U_C, V_C) \quad (3)$$

- The free-surface elevation is not nested (zero-gradient boundary condition)
- The barotropic velocity normal to the south boundary is computed according to a Flather type radiation condition (Flather, 1976), while the tangential velocity is set equal to the Alermo velocity.

$$\overline{V}_a = \overline{V}_{ac} - \sqrt{\frac{g}{H}}(\zeta - \zeta_C) \quad \text{and} \quad \overline{U}_a = \overline{U}_{ac} \quad (4)$$

where g is the acceleration of gravity and H the water column depth.

A volume constraint is applied on velocities normal to the open boundary to ensure that the water flux across the open boundary is the same with the one predicted by ALERMO.

2.3 Initial conditions and forcing

The model forcing employs 1-h atmospheric forecast fields at $1/10^\circ$ resolution, that were provided by the SKIRON (<http://forecast.uoa.gr/>) atmospheric Limited Area Model (LAM) which is based on a non-hydrostatic version of the ETA/NCEP model (<http://www.emc.ncep.noaa.gov/>). The asynchronous air-sea coupling is based on a well-tuned set of bulk formulae for the computation of momentum, heat and freshwater fluxes, taking the following atmospheric parameters as input:

1) Wind velocity at 10 m, 2) relative humidity at 2 m, 3) air temperature at 2 m, 4) precipitation, 5) net incoming short wave radiation and 6) incoming long wave radiation.

The net heat flux at the sea surface is given as the sum of radiative, sensible and evaporative components:

$$Q = Q_r - Q_e - Q_h \quad (5)$$

A nested circulation model for the North Aegean Sea

V. H. Kourafalou and
K. P. Tsiaras

Title Page

Abstract

Introduction

Conclusions

References

Tables

Figures

⏪

⏩

◀

▶

Back

Close

Full Screen / Esc

Printer-friendly Version

Interactive Discussion

where Q is the net heat flux to the ocean, Q_r is the net radiative gain received by the ocean, Q_h is the sensible heat flux and Q_e is the evaporative heat flux.

The radiative term Q_r in Eq. (1) consists of three components: the shortwave radiative gain received by the ocean Q_{rs} , the upward infrared radiation flux emitted by the ocean Q_{iru} and the downward atmospheric infrared radiation reaching the sea surface Q_{ird} :

$$Q = Q_{rs} - Q_{iru} + Q_{ird} \quad (6)$$

The net shortwave radiative gain at the sea surface Q_{rs} is provided directly by the atmospheric model at 1-h intervals. The downward infrared radiation flux term Q_{ird} is also provided directly by the atmospheric model at 1-h intervals while the upward infrared radiation flux term is estimated by the ocean model itself using the Stefan-Boltzman law:

$$Q_{iru} = \varepsilon \cdot \sigma \cdot T_s^4 \quad (7)$$

where ε , σ are the ocean emissivity (as given by Bignami et al., 1995) and the Stefan-Boltzman constant, respectively, and T_s is the sea surface temperature (predicted by the ocean model).

The evaporative Q_e and sensible Q_h heat flux terms are calculated by the ocean model using the bulk aerodynamic formulae (Rosati and Miyakoda, 1988; Castellari et al., 1998):

$$Q_e = \rho_A L_V C_E \left| \overline{W} \right| \left[e_{SAT}(T_S) - r e_{SAT}(T_A) \right] \frac{0.622}{\rho_A} \quad (8)$$

$$Q_h = \rho_A C_p C_H \left| \overline{W} \right| (T_S - T_A) \quad (9)$$

where the atmospheric data of wind speed $\left| \overline{W} \right|$ (at 10-m above sea surface), air temperature T_A and relative humidity r (at 2-m above sea surface) are provided by the atmospheric model at 1-hour intervals. The atmospheric saturation vapour pressure e_{SAT}

A nested circulation model for the North Aegean Sea

V. H. Kourafalou and
K. P. Tsiaras

Title Page

Abstract

Introduction

Conclusions

References

Tables

Figures

◀

▶

◀

▶

Back

Close

Full Screen / Esc

Printer-friendly Version

Interactive Discussion

in Eq. (4) is computed through a polynomial approximation as a function of temperature (Lowe, 1977). The specific heat capacity of air c_D and the atmospheric pressure at sea level p_A are considered as constants.

The sea surface temperature T_s is predicted by the hydrodynamic model itself, the density of moist air ρ_A is computed by the model as a function of air temperature and relative humidity and the latent heat of vaporization L_V is calculated as a function of sea surface temperature (Gill, 1982).

The turbulent exchange coefficients C_E and C_H are estimated in terms of air-sea temperature difference and the wind speed taking into account an atmospheric stability index (Kondo parameterisation – Kondo, 1975).

The virtual salt flux (*VSF*) surface boundary condition due to evaporation E and precipitation P is given by

$$VSF = (E - P) \cdot S \quad (10)$$

where S is the surface salinity predicted by the ocean model. Precipitation rates are provided by the atmospheric model at 1-h intervals while the evaporation rate is calculated from the evaporative heat flux using

$$E = \frac{Q_e}{L_V} \quad (11)$$

The calculation of the wind stress fields is based on the transformation of the 1-h wind velocity data at 10 m above sea surface to x and y components of wind stress following the formula:

$$\vec{\tau} = \rho_A C_D |\overline{W}| \overline{W} \quad (12)$$

where ρ_A is the density of moist air (computed by the ocean model as a function of air temperature and relative humidity), W is the wind velocity and C_D is the drag coefficient. The drag coefficient is calculated as a function of the wind speed and the air-sea temperature difference through the polynomial approximation given by Hellerman and Rosenstein (1983).

The initial conditions for Temperature, Salinity and Velocity as well as daily averaged fields along the open boundary were provided by the ALERMO model that performed the same simulation (initialized from the basin-wide MFSTEP Mediterranean OGCM) using the same atmospheric forcing.

3 Model simulations

The simulation described below was part of an experiment for several shelf and regional models within the MFSTEP project. The purpose was to test if shelf models can perform reliable short term simulations when initialized from a long running larger scale model simulation that also provides the boundary conditions. In addition, high frequency and high resolution atmospheric forcing was employed to enhance circulation features. This exercise did not involve data assimilation and was not intended to perform model validation through observations. It was rather an academic exercise intended to examine if the nested model could spin up from rest and be able to achieve circulation features present on the long-running larger scale model (with additional details due to the higher grid resolution) after a short (one month) period. The NAS shelf model simulated fields were compared to the ALERMO fields (which were taken as the closest to the “truth”), in order to test the nesting procedure, the air-sea coupling and the response of the higher resolution shelf model to the detailed atmospheric forcing.

The simulation period covered January 2003; the hourly LAM atmospheric forcing is illustrated in Figs. 3 and 4. Although the simulation period was short, the wind fields exhibited strong variability, both in time and space. As seen in Fig. 2, winds were strong, typical for the winter season, with the exception of the Northwestern basin of Thermaikos, where they tend to be lighter (see also Fig. 3). The wind direction had an extended period of southerlies at the beginning, turning into periods of northeasterlies that alternated with brief calm periods; an episode of southwesterlies occurred toward the end.

In general, the nesting procedure performed well, as circulation patterns computed

A nested circulation model for the North Aegean Sea

V. H. Kourafalou and
K. P. Tsiaras

Title Page

Abstract

Introduction

Conclusions

References

Tables

Figures

⏪

⏩

◀

▶

Back

Close

Full Screen / Esc

Printer-friendly Version

Interactive Discussion

by ALERMO and the NAS shelf model were compatible near the open boundary. We performed a series of sensitivity tests, using the ALERMO fields as an academic “validation” tool. The most effective changes involved vertical resolution (16 and 25 layers) and the specification of the ALERMO velocity V_{init} in the calculation of initial fields (in addition to the T and S fields). We present the weekly averaged fields at the end of the integration period for three different simulations (Figs. 5a–c) and the corresponding ALERMO field (Fig. 5d). We also present the sea surface height difference between the two models in Fig. 6. In general, we see smaller scale features developed in the shelf model and absent in ALERMO, as expected, due to the higher shelf model resolution. However, we focus on larger scale features, which should appear more similar. Figures 5a and c show the results from two different initialization procedures. Starting from some discrepancies between the two models when vertical resolution was lower and no V_{init} was included (Case I, Fig. 5a), we achieved better agreement by increasing the number of vertical layers from 16 to 25 (Case II, Fig. 5b). For instance, the cyclone in the Sporades basin is strengthened and an eddy forms south of the Lesvos island. The circulation in the deep basins of the shelf model (not shown) acquires greater similarity to ALERMO, which we attribute to the improvement in the middle and lower level circulation, due to higher vertical resolution. When the ALERMO velocity fields V_{init} were not used (Fig. 5a, b), certain mesoscale features in the deeper basins along the North Aegean trough (Sporades and Athos basins) are not as well developed in the shelf model. This is attributed to the short integration time of the MFSTEP experiment. When the ALERMO velocity fields were used for initialization (Case III), the similarity to ALERMO improved, as is evident from the overall better agreement in the eddy field (Fig. 5c). This improvement is also evident from Fig. 6, where differences in the Sporades basin were minimized and differences were reduced in a number of other areas. However, differences remained to the north and northeast of the Lemnos island, as this is the area mostly affected by the Dardanelles inflow. As we will discuss below, this is an area where the salinity fields for the two models are most diverse.

The use of the ALERMO velocity fields for initialization increased the overall eddy

A nested circulation model for the North Aegean Sea

V. H. Kourafalou and
K. P. Tsiaras

[Title Page](#)[Abstract](#)[Introduction](#)[Conclusions](#)[References](#)[Tables](#)[Figures](#)[⏪](#)[⏩](#)[◀](#)[▶](#)[Back](#)[Close](#)[Full Screen / Esc](#)[Printer-friendly Version](#)[Interactive Discussion](#)

kinetic energy in the shelf model. This is largely due to the strengthening of the deep shelf circulation. Upper level features were also affected, as shown in Fig. 7 where the daily averaged velocity fields at 10 m are exhibited for the Case I, Case III and ALERMO simulations at the last day of integration (30 January 2003). The best qualitative agreement to ALERMO is for Case III, but both Case I and Case III exhibit overall more active eddy fields.

In Fig. 8 we compare the basin wide mean kinetic energy for the above experiments. In addition, we include one more ALERMO experiment that was continuous for 2002 and 2003 as a reference. Although the two ALERMO experiments were nested on different basin-wide Mediterranean models (Modular Ocean Model, MOM, for the longer simulations versus OPA for the January 2003 period), they both achieve the same mean kinetic energy time series during the common month, after an initialization period of about 6 days for the simulation that started on 1 January 2003. For the NAS experiments, it took a spin-up period of about 8 days for Case II and 5 days for Case III, but they both acquired higher mean kinetic energy during the period of persistent and rather weak northerlies until they merged with the ALERMO time series toward the end of the month, right after the maximum winds (~25 January) and the shift to the southerly direction. The higher mean kinetic energy in the NAS experiments is the cumulative result of several small eddies that are absent in the coarser ALERMO domain.

The NAS model simulated surface temperature patterns are quite similar to the ALERMO patterns. As seen in the weekly averaged distribution in Fig. 9, somewhat lower temperature values ($<0.8^{\circ}\text{C}$) are found in the coastal areas due to the lower shelf model minimum depth (10 m) as compared to the ALERMO minimum coastal depth (26 m). As expected for winter, the temperature gradients are mainly North-South, rather than East-West as is common for summer (Kourafalou and Barbopoulos, 2003). The model values in the Thermaikos Gulf seem reasonable for winter, as deduced from in-situ measurements in other years (Kontoyiannis et al., 2003).

Salinity patterns of the NAS model (Fig. 10) are quite similar to the ALERMO fields,

A nested circulation model for the North Aegean Sea

V. H. Kourafalou and
K. P. Tsiaras

[Title Page](#)[Abstract](#)[Introduction](#)[Conclusions](#)[References](#)[Tables](#)[Figures](#)[◀](#)[▶](#)[◀](#)[▶](#)[Back](#)[Close](#)[Full Screen / Esc](#)[Printer-friendly Version](#)[Interactive Discussion](#)

A nested circulation model for the North Aegean Sea

V. H. Kourafalou and
K. P. Tsiaras

[Title Page](#)[Abstract](#)[Introduction](#)[Conclusions](#)[References](#)[Tables](#)[Figures](#)[⏪](#)[⏩](#)[◀](#)[▶](#)[Back](#)[Close](#)[Full Screen / Esc](#)[Printer-friendly Version](#)[Interactive Discussion](#)

but with somewhat more pronounced coastal features, due to the enhanced coastal currents. This is due to the lower coastal depths, the sharper slope near the coast (all factors influencing the wind-driven coastal current component) plus the inclusion of additional rivers (Evros, Pinios and Nestos that are absent in ALERMO, see Fig. 1), a factor that affects the buoyancy-driven component. The most pronounced changes were found in the pathways of the waters of Black Sea origin (BSW), which form the Dardanelles buoyant plume. Even though the parameterization of BSW inflow at the Dardanelles is the same, the inflow velocity field and consequently the simulated buoyant plume can vary, due to subtle topographic details, the result of the different resolution and minimum coastal depth.

We examine the effect of changes in the high frequency/high resolution wind field on the areas affected by buoyant discharges (mainly the Dardanelles plume area and the Northwestern shelf in the Gulf of Thermaikos). During the first 10 days, southerly winds dominate (Figs. 2, 3) which are downwelling-favourable for the east Aegean coast and greatly restrict the Dardanelles plume, but they are upwelling-favourable for the west coast and they allow offshore expansion of the low salinity band in the Thermaikos Gulf. The relaxation of the wind field in the middle of the month allows the release of low salinity waters in the vicinity of the Dardanelles and through the Lemnos plateau. The winds are almost negligible in the Gulf of Thermaikos, allowing the formation of a southward buoyancy-driven coastal current there that starts from the Axios River and continues to the south of the Pinios River. When the winds attain a strong northerly component everywhere (around the 25th), the Thermaikos coastal current is strengthened, as it is now both buoyancy and wind driven, while coastal currents are evident on other Northern Aegean shelf areas. The pool of low salinity waters that was advected on the Lemnos plateau gets quickly mixed with the ambient waters, while the core of the Dardanelles plume starts to retreat and is again found confined near the Dardanelles Straits by the end of the month (30/1), when winds have shifted to southerlies. On the same day, an intrusion of higher salinity Aegean waters is evident in the Thermaikos Gulf.

A nested circulation model for the North Aegean Sea

V. H. Kourafalou and
K. P. Tsiaras

In order to examine the effect of a longer simulation on model computed fields for January 2003, we utilized ALERMO fields from the continuous 2002–2003 simulation depicted in Fig. 8, to initialize the NAS model on 2 September 2002 and run with the same (coarser) atmospheric fields until 2 January 2003, when we imposed the LAM fields as before. Consequently, the simulations during January 2003 were identical, with the exception of the initial fields. In the new simulation, we initialized from the temperature and salinity fields (no velocity) of 1 January 2003 from the simulation that started on 2 September 2002. We observed that the NAS model was capable to establish an overall enhanced current field (as compared to the Case I experiment, that did not have velocity in the initial condition), as the longer initialisation period allowed the full development of circulation features. In addition, submesoscale eddies were also enhanced, as they were not suppressed by the imposition of the coarser ALERMO velocity fields. The river plumes and the Dardanelles plume also appeared more developed. This suggests that short term simulations of downscaled nested shelf (NAS) and regional (ALERMO) models in areas of high variability as the Aegean Sea might not allow the full development of circulation features, a problem that does not appear to be overcome by employing high resolution atmospheric fields.

4 Concluding remarks

The modeling of the entire North Aegean in very fine resolution (1 min or ~ 1.6 km) and under atmospheric forcing that allows temporal and spatial details (1-h forcing from an atmospheric Limited Area Model of ~ 9 km resolution) has been performed for the first time in the framework of the MFSTEP project.

The shelf and coastal areas in the North Aegean model domain exhibited a rapid response to the variability of the atmospheric forcing. The wind was a major circulation driving mechanism during January 2003, as is common for the winter season. The high frequency variability in the wind input resulted in rapidly shifting coastal currents and remarkable changes in the advection of low salinity waters within areas affected by the

[Title Page](#)[Abstract](#)[Introduction](#)[Conclusions](#)[References](#)[Tables](#)[Figures](#)[⏪](#)[⏩](#)[◀](#)[▶](#)[Back](#)[Close](#)[Full Screen / Esc](#)[Printer-friendly Version](#)[Interactive Discussion](#)

river plumes and around the Dardanelles plume. Despite the short integration period, forcing variability was substantial, as the wind field changed from strong southerlies in early January to strong northerlies in late January with a wind relaxation period in between and with a return to southerlies by the end of the month. Spatial variability in the wind field was also observed, especially for the Gulf of Thermaikos area (Northwest Aegean shelf), where winds were weaker and generally different in their east-west component, as compared to the rest of the domain.

This paper did not attempt a model validation with observations (that were sparse during this period) but a comparison to fields from the larger scale ALERMO model to determine the best approach in nesting procedure, the effects of atmospheric forcing of high resolution in time and space and the overall feasibility of such short term simulations, in preparation for future forecasts. We found that the results that compared best with ALERMO were reached with high vertical resolution and the employment of the outer model velocities along with the T and S fields during the initialization procedure. We attributed this to the short period of the experiment which prevents the model from computing a fully developed velocity field from the imposed density field. By performing an experiment with a longer initialization period, we found that, at least for the North Aegean, this is a preferable strategy that avoids the need for prescribed velocity fields from the outer model, a procedure that may suppress fine scale details of the nested model velocity field. As this is not practical for operational purposes, an update of the boundary conditions for velocity is suggested during coupled forecasting simulations, at a frequency that has to be determined for optimal results. A longer term simulation for 2002–2003 is currently under way, that will cover periods when observations are available to fully evaluate the high resolution, nested NAS model.

The two areas that are mostly influenced by buoyant discharges, namely the Gulf of Thermaikos and the Dardanelles plume (around the Lemnos island) were discussed in terms of salinity changes caused by the influence of wind on the surface advected plumes. We should caution that all North Aegean rivers and the Dardanelles inflow were “climatological” values, not necessarily representative of the January 2003 con-

A nested circulation model for the North Aegean Sea

V. H. Kourafalou and
K. P. Tsiaras

[Title Page](#)[Abstract](#)[Introduction](#)[Conclusions](#)[References](#)[Tables](#)[Figures](#)[⏪](#)[⏩](#)[◀](#)[▶](#)[Back](#)[Close](#)[Full Screen / Esc](#)[Printer-friendly Version](#)[Interactive Discussion](#)

ditions, as no such information was available. However, we focused on the study of certain processes, especially the simulated rapid changes in coastal flows and river plumes, in response to the varying wind conditions. The coastal current along the western Thermaikos and the changes in width and alongshore extension due to wind effects has been previously documented in a study that combined observations and modelling to discuss the related processes and their seasonal variability (Kontoyianis et al., 2003). Here, we showed that similar changes can be expected in shorter time periods, due to episodic changes in wind forcing. For the Dardanelles plume, the NAS and the ALERMO models exhibited the strongest differences in salinity and velocity patterns. This was attributed to differences in topographic details near the Dardanelles, which, although small, influenced the transport rates and pathways of the buoyant waters through the island passages. This is an important finding, as details in the initial distribution of the Dardanelles plume may influence the pathways of this strongest lateral buoyant input for the North Aegean, with implications on the general circulation in the area and possibly influencing water properties in the entire Aegean Sea. The future development of a North Aegean model for forecast purposes requires details in river discharges and a parameterization of the Dardanelles flow exchange based on comprehensive direct measurements.

Acknowledgements. The study was supported by the EU funded MFSTEP project (contract # EVK3-CT-2002-00075). We appreciate the collaboration with all colleagues in the modeling group of the MFSTEP project.

References

- Balopoulos, E. T., Collins, M. B., and James, A. E.: Residual circulation in a coastal embayment of the Eastern Mediterranean Sea (Thermaikos Bay, N.W. Aegean), *Thalassographica*, 9, 7–22, 1986.
- Biglami, F., Marullo, S., Santoleri, R., and Schiano, M. E.: Longwave radiation budget in the Mediterranean Sea, *J. Geophys. Res.*, 100(C2), 2501–2514, 1995.

A nested circulation model for the North Aegean Sea

V. H. Kourafalou and
K. P. Tsiaras

Title Page

Abstract

Introduction

Conclusions

References

Tables

Figures

⏪

⏩

◀

▶

Back

Close

Full Screen / Esc

Printer-friendly Version

Interactive Discussion

A nested circulation model for the North Aegean Sea

V. H. Kourafalou and
K. P. Tsiaras

[Title Page](#)[Abstract](#)[Introduction](#)[Conclusions](#)[References](#)[Tables](#)[Figures](#)[⏪](#)[⏩](#)[◀](#)[▶](#)[Back](#)[Close](#)[Full Screen / Esc](#)[Printer-friendly Version](#)[Interactive Discussion](#)

- Blumberg, A. F. and Mellor, G. L.: Diagnostic and prognostic numerical circulation studies of the South Atlantic Bight, *J. Geophys. Res.*, 88(C8), 4579–4592, 1983.
- Castellari, S., Pinardi, N., and Leaman, K.: A model study of air-sea interactions in the Mediterranean Sea, *J. Mar. Syst.*, 18, 89–114, 1998.
- 5 Demirov, E. and Pinardi, N.: Simulation of the Mediterranean Sea circulation from 1979 to 1993. Part I: The interannual variability, *J. Mar. Sys.*, 33/34, 23–50, 2002.
- Flather, R. A.: A tidal model of the northwest European continental shelf, *Memoires Societe Royale des Sciences de Liege, Series 6 (10)*, 141–164, 1976.
- Gill, A. E.: *Atmosphere-Ocean Dynamics*, Academic Press, New York, 662 pp., 1982.
- 10 Hellermann, S. and Rosenstein, M.: Normal wind stress over the world ocean with error estimates, *J. Phys. Oceanogr.*, 13, 1093–1104, 1983.
- Karageorgis, A. P., Kaberi, H. G., Tengberg, A., Zervakis, V., Hall, P. O. J., and Anagnostou, Ch. L.: Comparison of particulate matter distribution, in relation to hydrography, in the mesotrophic Skagerrak and the oligotrophic northeastern Aegean Sea, *Continental Shelf Research*, 23, 1787–1809, 2003.
- 15 Kondo, J.: Air-sea bulk transfer coefficients in diabatic conditions, *Boundary-Layer Meteorol.*, 9, 91–112, 1975.
- Kontoyiannis, H., Kourafalou, V. H., and Papadopoulos, V.: The seasonal characteristics of the hydrology and circulation in the Northwest Aegean Sea (Eastern Mediterranean): observations and modeling, *J. Geophys. Res.*, 108(C9), 3302, doi:10.1029/2001JC001132, 2003.
- 20 Korres, G., Laskaratos, A., and Hatzia Apostolou, E.: Towards an ocean forecasting system for the Aegean Sea, *The Global Atmosphere and Ocean System*, 8(2–3), 173–200, 2002.
- Kourafalou, V. H., Oey, L.-Y., Wang, J. D., and Lee, T. N.: The fate of river discharge on the continental shelf. Part I: modelling the river plume and the inner-shelf coastal current, *J. Geophys. Res.*, 101(C2), 3415–3434, 1996.
- 25 Kourafalou, V. H. and Barbopoulos, K.: High resolution simulations on the North Aegean Sea seasonal circulation, *Ann. Geophys.*, 21, 251–265, 2003.
- Kourafalou, V. H., Savvidis, Y. G., Koutitas, C. G., and Krestenitis, Y. N.: Modeling studies on the processes that influence matter transfer on the Gulf of Thermaikos (NW Aegean Sea), *Continental Shelf Research*, 24, 203–222, 2004.
- 30 Lowe, P. R.: An approximating polynomial for the computation of saturation vapor pressure, *J. Appl. Meteorol.*, 16, 100–103, 1977.
- Mellor, G. L. and Yamada, T.: Development of a turbulence closure model for geophysical fluid

A nested circulation model for the North Aegean Sea

V. H. Kourafalou and
K. P. Tsiaras

[Title Page](#)[Abstract](#)[Introduction](#)[Conclusions](#)[References](#)[Tables](#)[Figures](#)[⏪](#)[⏩](#)[◀](#)[▶](#)[Back](#)[Close](#)[Full Screen / Esc](#)[Printer-friendly Version](#)[Interactive Discussion](#)

problems, *Rev. Geophys. Space Phys.*, 20(4), 851–875, 1982.

Nittis, K., Zervakis, V., Papageorgiou, E., and Perivoliotis, L.: Atmospheric and Oceanic observations from the POSEIDON buoy network: Initial results, *The Global Atmosphere and Ocean System*, special issue – POSEIDON: An Integrated Operational Oceanographic System, 8(2-3), 87–99, 2002.

Nittis, K., Perivoliotis, L., Korres, G., Tziavos, C., and Thanos, I.: Operational monitoring and forecasting for marine environmental applications in the Aegean Sea, *Environmental Modelling and Software*, 21, 243–257, 2006.

Pinardi, N., Allen, I., Demirov, E., De Mey, P., Korres, G., Lascaratos, A., Le Traon, P.-Y., Maillard, C., Manzella, G., and Tziavos, C.: The Mediterranean Ocean Forecasting System: First phase of implementation (1998–2001), *Ann. Geophys.*, 21, 3–20, 2003.

Poulos, S. E., Drakopoulos, P. G., and Collins, M. B.: Seasonal variability in sea surface oceanographic conditions in the Aegean Sea (Eastern Mediterranean): an overview, *J. Mar. Sys.*, 13, 225–244, 1997.

Rosati, A. and Miyakoda, K.: A general circulation model for upper ocean circulation, *J. Phys. Oceanogr.*, 18, 1601–1626, 1988.

Smagorinsky, J.: General circulation experiments with the primitive equations, I. The basic experiment, *Mon. Wea. Rev.*, 91, 99–164, 1963.

Therianos, A. D.: Rainfall and geographical distribution of river runoff in Greece, *Bull. Geol. Soc. Greece*, XI, 28–58 (in Greek), 1974.

Zervakis, V., Georgopoulos, D., and Drakopoulos, P. G.: The role of the North Aegean in triggering the recent Eastern Mediterranean climate changes, *J. Geophys. Res.*, 105, 26 103–26 116, 2000.

Zervakis, V. and Georgopoulos, D.: Hydrology and Circulation in the North Aegean (eastern Mediterranean) throughout 1997–1998, *Mediterranean Marine Science*, 3(1), 7–21, 2002.

Zodiatis, G. and Balopoulos, E.: Structure and characteristics of fronts in the North Aegean Sea, *Boll. Oceanol. Theor. Appl.*, XI, 113–124, 1993.

Zodiatis, G.: Advection of the Black Sea water in the north Aegean Sea, *Global Atmos. Ocean Syst.*, 2, 41–60, 1994.

Zodiatis, G., Alexandri, S., Pavlakis, P., Jönsson, L., Kallos, G., Demetropoulos, A., Georgiou, G., Theodorou, A., and Balopoulos, E.: Tentative study of flow patterns in the North Aegean Sea using NOAA-AVHRR images and 2D model simulations, *Ann. Geophys.*, 14, 1221–1231, 1996.

A nested circulation model for the North Aegean Sea

V. H. Kourafalou and
K. P. Tsiaras

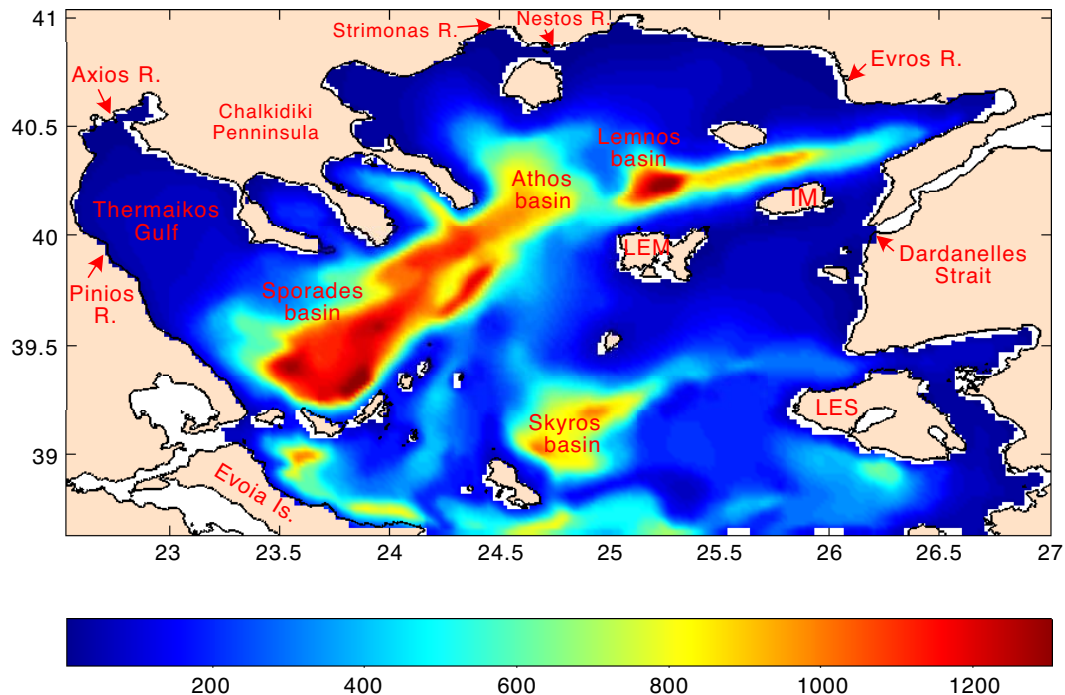


Fig. 1. The bathymetry of the North Aegean Sea (NAS) model, sub-basins and rivers. LES: Lesvos island; LE: Lemnos island; IM: Imroz island.

Title Page

Abstract

Introduction

Conclusions

References

Tables

Figures

◀

▶

◀

▶

Back

Close

Full Screen / Esc

Printer-friendly Version

Interactive Discussion

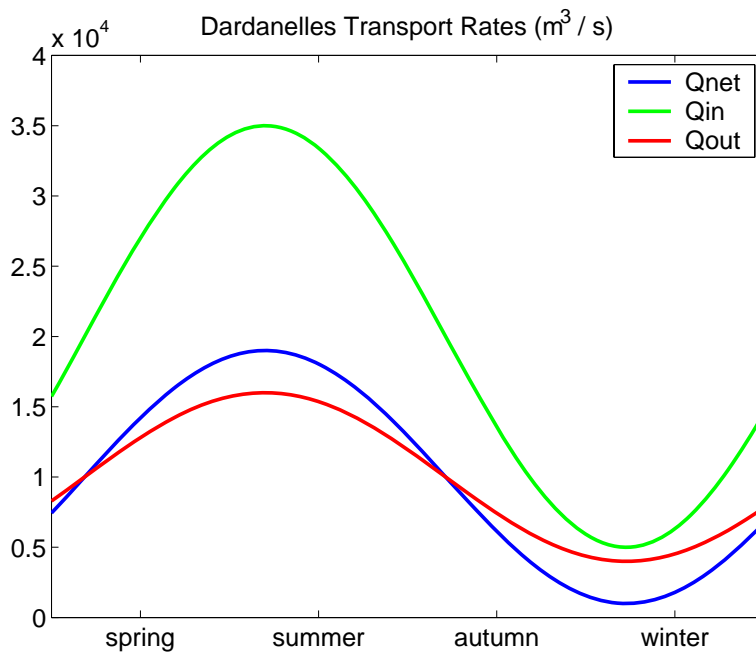
A nested circulation model for the North Aegean SeaV. H. Kourafalou and
K. P. Tsiaras

Fig. 2. The annual distribution of Dardanelles inflow (Q_{in}), outflow (Q_{out}) and net flux (Q_{net}), as prescribed for the NAS and ALERMO models.

[Title Page](#)[Abstract](#)[Introduction](#)[Conclusions](#)[References](#)[Tables](#)[Figures](#)[◀](#)[▶](#)[◀](#)[▶](#)[Back](#)[Close](#)[Full Screen / Esc](#)[Printer-friendly Version](#)[Interactive Discussion](#)

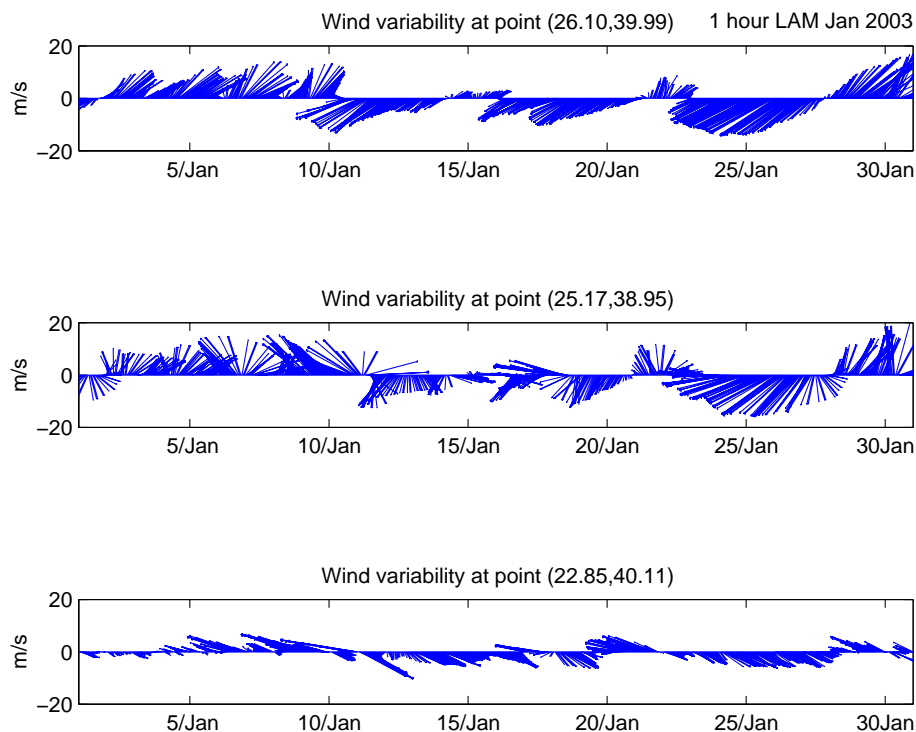
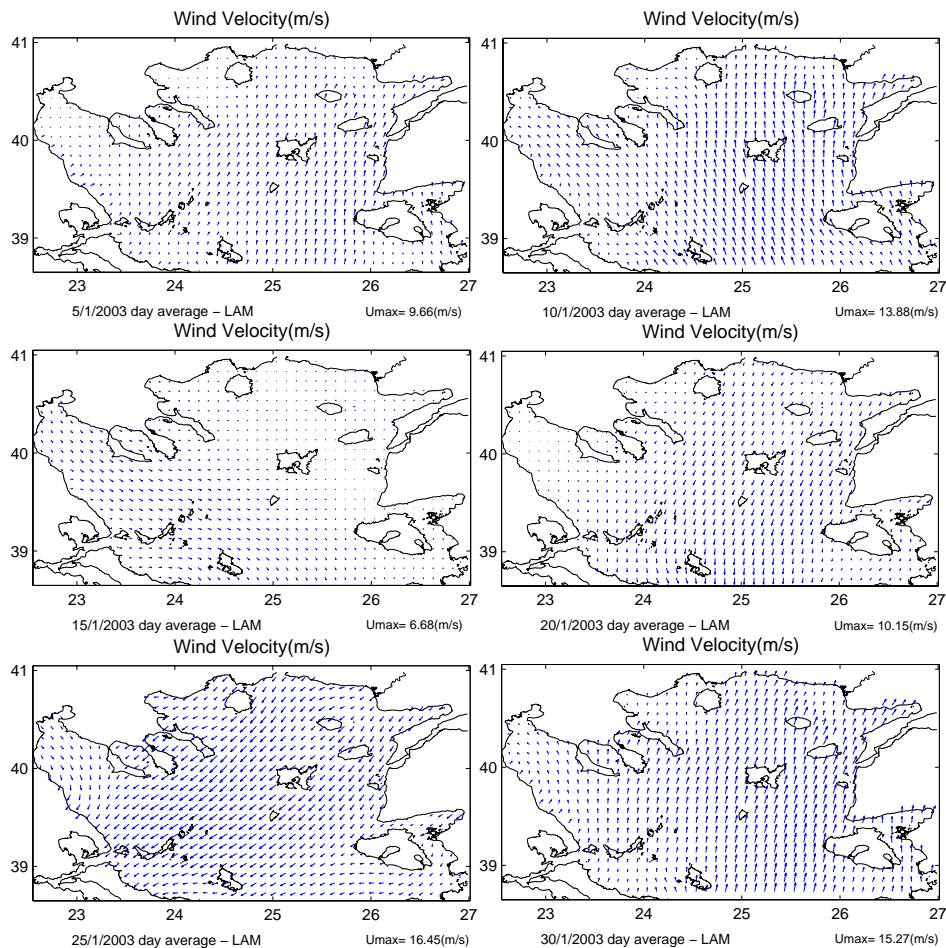
A nested circulation model for the North Aegean SeaV. H. Kourafalou and
K. P. Tsiaras

Fig. 3. Limited Area Model (LAM) atmospheric forcing time series for January 2003 at 3 points of the NAS domain; near the Dardanelles (upper); near the south NAS boundary (middle) and in the Thermaikos Gulf (bottom).

[Title Page](#)[Abstract](#)[Introduction](#)[Conclusions](#)[References](#)[Tables](#)[Figures](#)[◀](#)[▶](#)[◀](#)[▶](#)[Back](#)[Close](#)[Full Screen / Esc](#)[Printer-friendly Version](#)[Interactive Discussion](#)

A nested circulation model for the North Aegean SeaV. H. Kourafalou and
K. P. Tsiaras**Fig. 4.** Horizontal distribution of winds on January 2003 (5 day interval).[Title Page](#)[Abstract](#)[Introduction](#)[Conclusions](#)[References](#)[Tables](#)[Figures](#)[◀](#)[▶](#)[◀](#)[▶](#)[Back](#)[Close](#)[Full Screen / Esc](#)[Printer-friendly Version](#)[Interactive Discussion](#)

A nested circulation model for the North Aegean Sea

V. H. Kourafalou and
K. P. Tsiaras

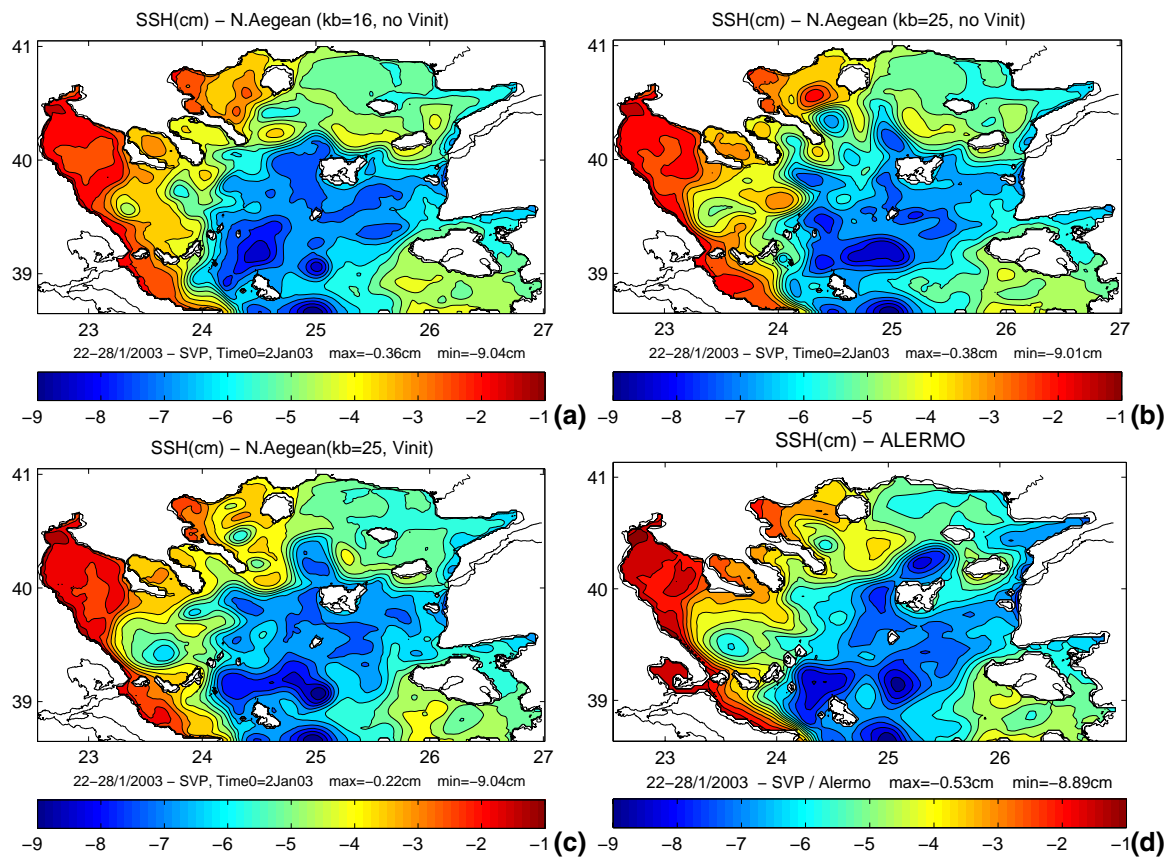


Fig. 5. Sea surface height weekly averaged for 22–28 January 2003 as simulated by (a) the N. Aegean model (kb=16, no Vinit); (b) the N. Aegean model (kb=25, no Vinit); (c) the N. Aegean model (kb=25, Vinit); (d) the ALERMO model.

[Title Page](#)
[Abstract](#)
[Introduction](#)
[Conclusions](#)
[References](#)
[Tables](#)
[Figures](#)
[Back](#)
[Close](#)
[Full Screen / Esc](#)
[Printer-friendly Version](#)
[Interactive Discussion](#)

A nested circulation model for the North Aegean Sea

V. H. Kourafalou and
K. P. Tsiaras

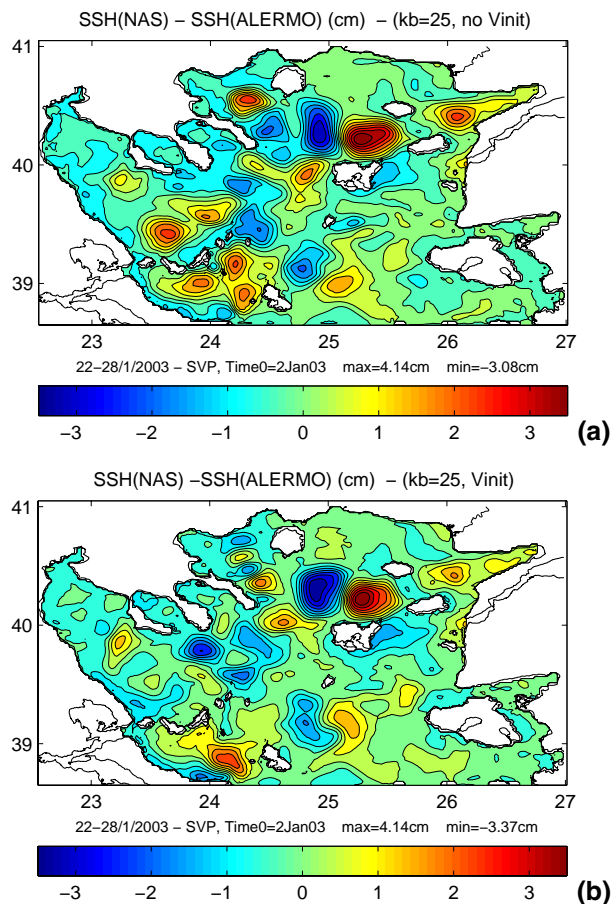


Fig. 6. Difference in the simulated sea surface height between the nested **(a)** NAS model (kb=25, no Vinit); **(b)** NAS model (kb=25, Vinit) and the outer ALERMO model: SSH(NAS)-SSH(ALERMO), averaged for 22–28 January.

[Title Page](#)[Abstract](#)[Introduction](#)[Conclusions](#)[References](#)[Tables](#)[Figures](#)[◀](#)[▶](#)[◀](#)[▶](#)[Back](#)[Close](#)[Full Screen / Esc](#)[Printer-friendly Version](#)[Interactive Discussion](#)

A nested circulation model for the North Aegean Sea

V. H. Kourafalou and
K. P. Tsiaras

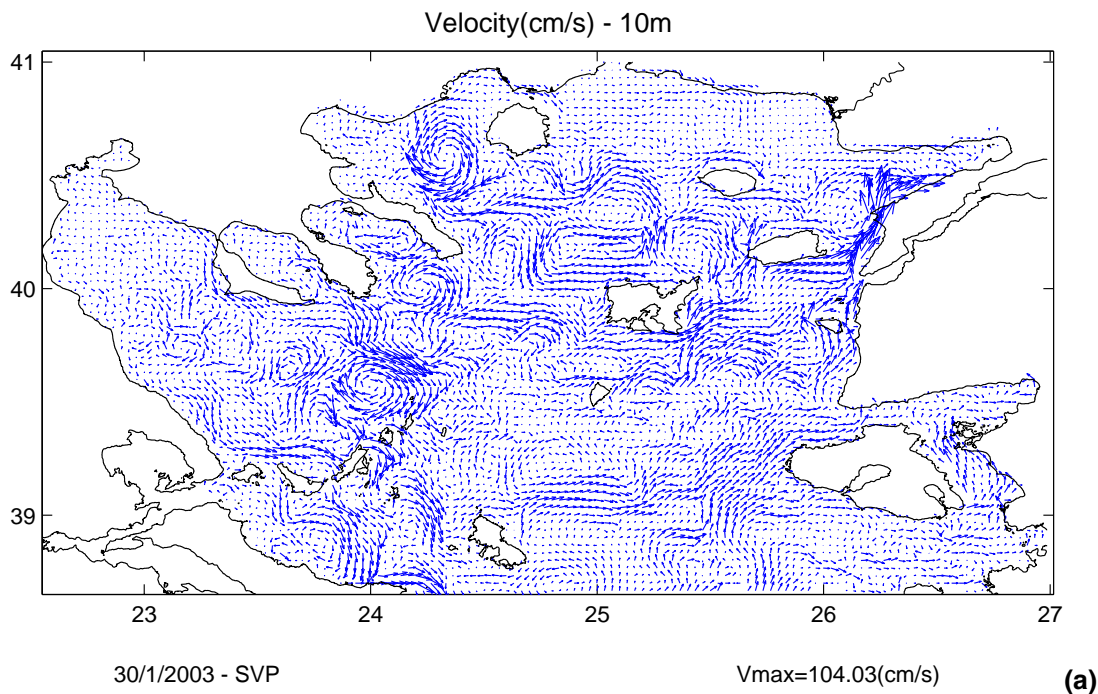
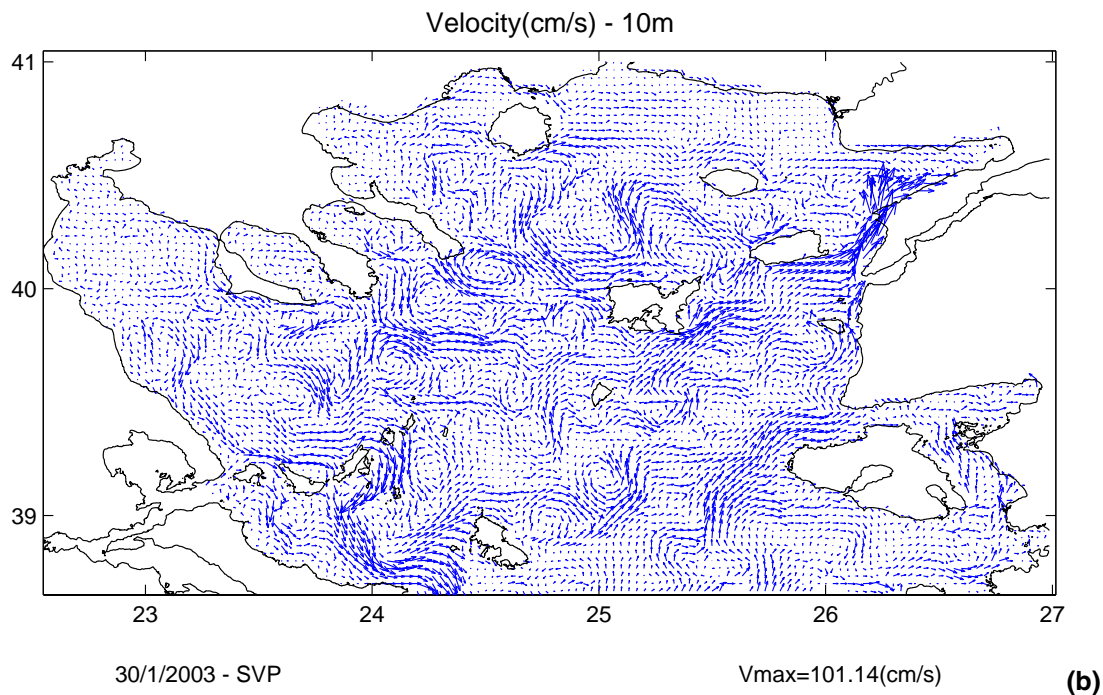
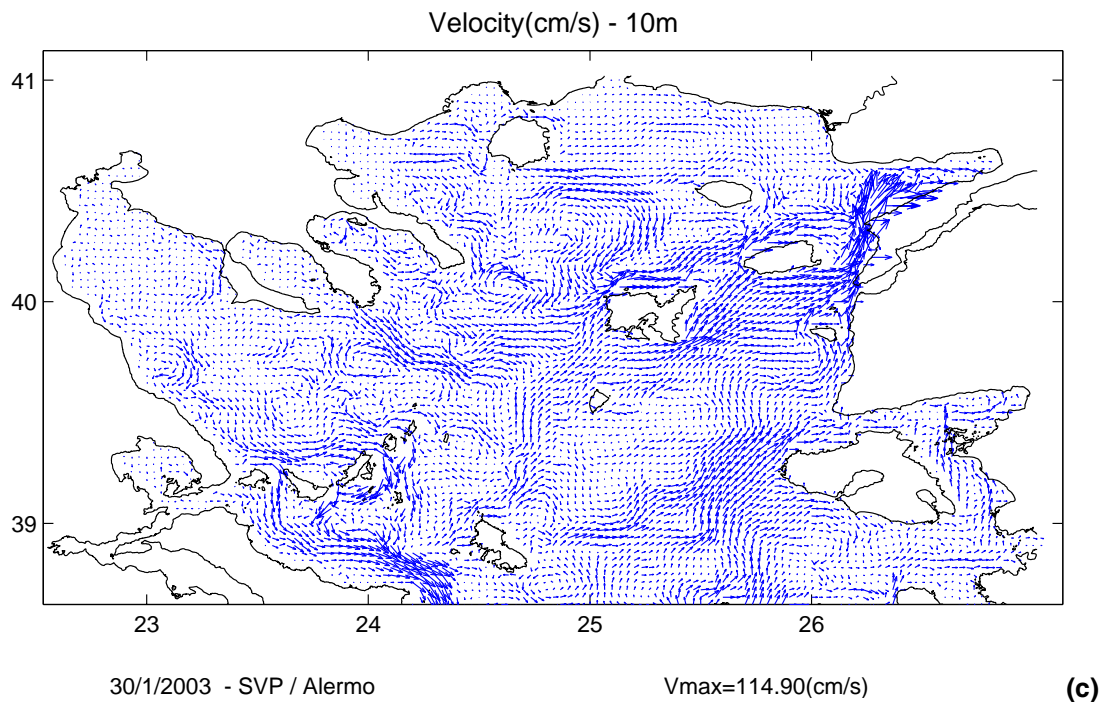


Fig. 7. Velocity fields at 10 m calculated from the NAS Case II experiment (a), the NAS Case III experiment (b) and the ALERMO (c), averaged over the last day of the simulation (30 January 2003).

[Title Page](#)[Abstract](#)[Introduction](#)[Conclusions](#)[References](#)[Tables](#)[Figures](#)[◀](#)[▶](#)[◀](#)[▶](#)[Back](#)[Close](#)[Full Screen / Esc](#)[Printer-friendly Version](#)[Interactive Discussion](#)

**A nested circulation
model for the North
Aegean Sea**V. H. Kourafalou and
K. P. Tsiaras**Fig. 7.** Continued.[Title Page](#)[Abstract](#)[Introduction](#)[Conclusions](#)[References](#)[Tables](#)[Figures](#)[◀](#)[▶](#)[◀](#)[▶](#)[Back](#)[Close](#)[Full Screen / Esc](#)[Printer-friendly Version](#)[Interactive Discussion](#)

A nested circulation model for the North Aegean SeaV. H. Kourafalou and
K. P. Tsiaras**Fig. 7.** Continued.

Title Page

Abstract

Introduction

Conclusions

References

Tables

Figures

◀

▶

◀

▶

Back

Close

Full Screen / Esc

Printer-friendly Version

Interactive Discussion

A nested circulation model for the North Aegean Sea

V. H. Kourafalou and
K. P. Tsiaras

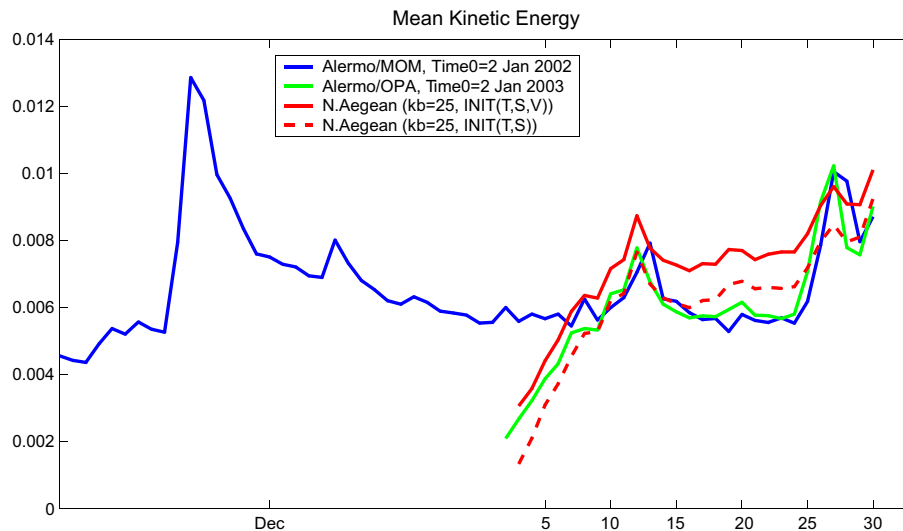


Fig. 8. Kinetic energy of the ALERMO Interannual simulation (blue line), the ALERMO SVP simulation (green line), the N. Aegean model with specified Vinit (red line) and without (red dash line).

Title Page

Abstract

Introduction

Conclusions

References

Tables

Figures

◀

▶

◀

▶

Back

Close

Full Screen / Esc

Printer-friendly Version

Interactive Discussion

A nested circulation model for the North Aegean Sea

V. H. Kourafalou and
K. P. Tsiaras

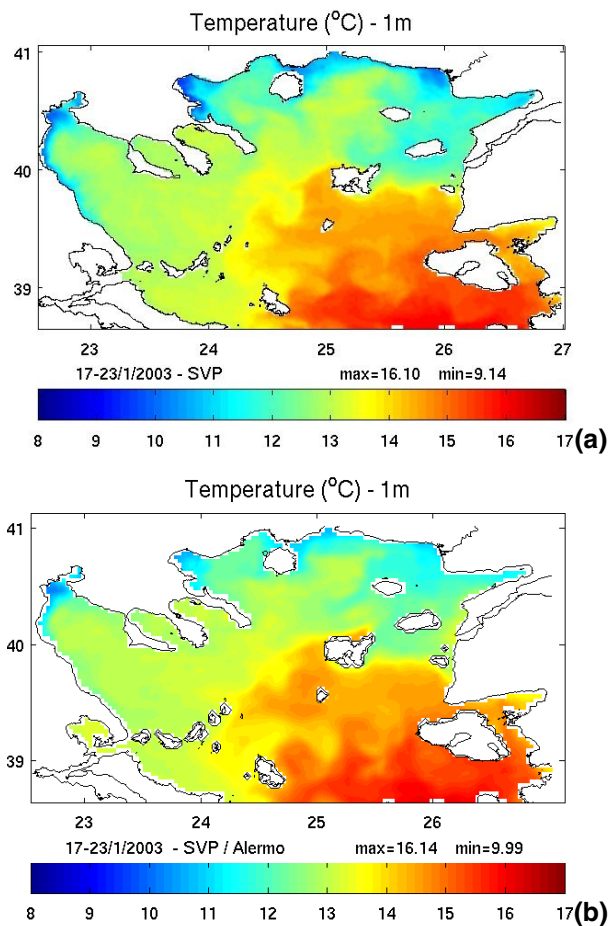


Fig. 9. Sea surface temperature weekly averaged for 17–23 January 2003 as simulated by (a) the N. Aegean model and (b) as simulated by the ALERMO model.

[Title Page](#)[Abstract](#)[Introduction](#)[Conclusions](#)[References](#)[Tables](#)[Figures](#)[◀](#)[▶](#)[◀](#)[▶](#)[Back](#)[Close](#)[Full Screen / Esc](#)[Printer-friendly Version](#)[Interactive Discussion](#)

A nested circulation model for the North Aegean Sea

V. H. Kourafalou and
K. P. Tsiaras

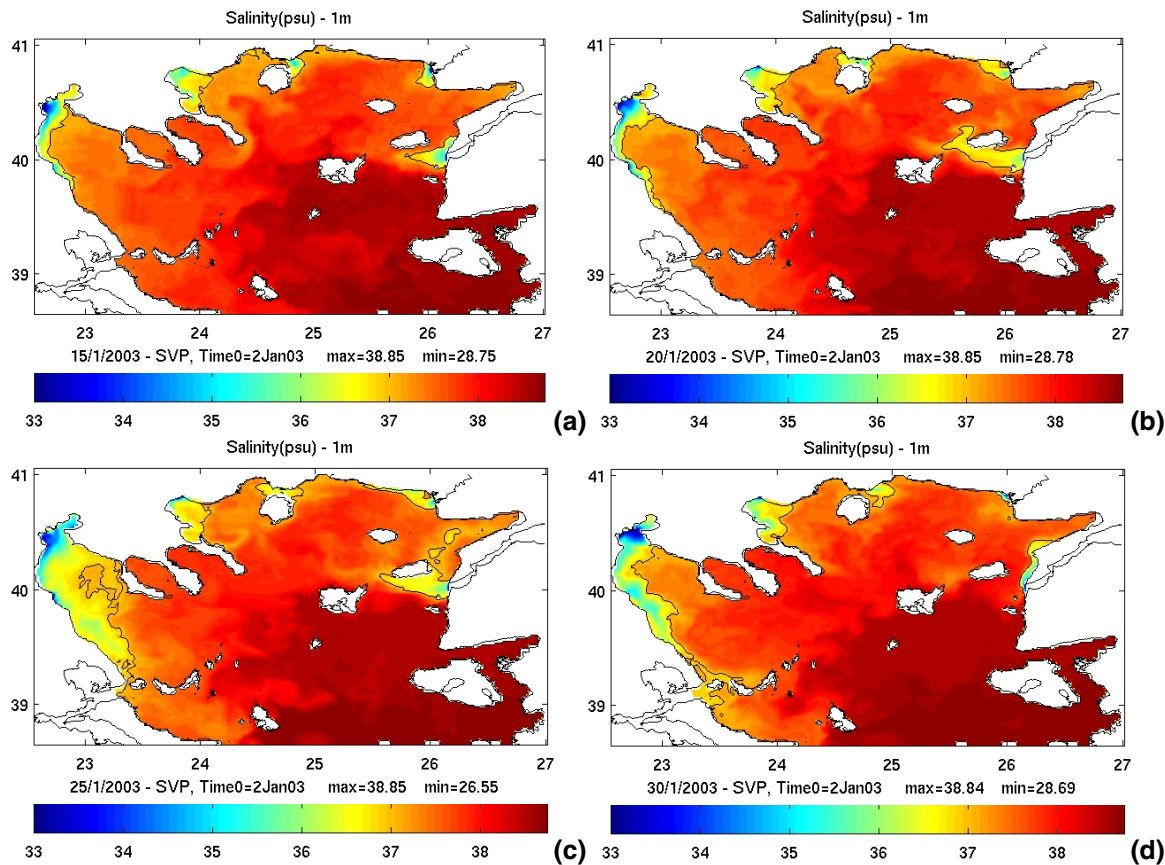


Fig. 10. Daily averaged, model simulated near surface salinity for N. Aegean on (a) 15 January 2003; (b) 20 January 2003; (c) 25 January 2003 and (d) 30 January 2003; the contour line marks the 37 isohaline.

Title Page

Abstract

Introduction

Conclusions

References

Tables

Figures

◀

▶

◀

▶

Back

Close

Full Screen / Esc

Printer-friendly Version

Interactive Discussion